Title	**Flat-top MZI filters: A novel robust design based on MMI splitters**
Author(s)	Cherchi, Matteo; Harjanne, Mikko; Ylinen, Sami; Kapulainen, Markku; Vehmas, Tapani; Aalto, Timo
Citation	Proceedings of SPIE. Vol. 9752, 9 pages
Date	2016
URL	DOI: 10.1117/12.2210937
Rights	Copyright 2016 Society of Photo Optical Instrumentation Engineers (SPIE). One print or electronic copy may be made for personal use only. Systematic reproduction and distribution, duplication of any material in this publication for a fee or for commercial purposes, or modification of the contents of the publication are prohibited.

Flat-top MZI filters: a novel robust design based on MMI splitters

Matteo Cherchi*, Mikko Harjanne, Sami Ylinen,
Markku Kapulainen, Tapani Vehmas, and Timo Aalto
VTT Technical Research Centre of Finland, Tietotie 3, 02150 Espoo, Finland

Keywords: Photonic Integrated Circuits, Integrated Optics, Silicon Photonics, WDM filters, Multimode interference splitters.

ABSTRACT

Multimode Interferometers (MMIs) are an attractive alternative to directional couplers, ensuring more relaxed tolerances to fabrication errors and broader operation bandwidth. The drawback is that only a limited discrete set of splitting ratios is achievable with MMIs of constant cross section. This issue clearly limits their use in flat-top interferometric filters, which design requires, in general, free choice of the splitting ratios. Here we show for the first time that it is possible to design 4-stage flat-top interferometers using only standard MMIs with 50:50 and 85:15 splitting ratios. The design approach is based on the representation of the system on the Bloch sphere. Flat-top interleavers with different free spectral ranges have been designed and fabricated on the silicon photonics platform of VTT, based on 3 µm thick rib and strip waveguides. Two different layouts have been explored: one where all components are collinear and a more compact one which elements have been folded in a spiral shape. All interleavers have been designed for TE polarization, and they work in a wavelength range comparable with the 100 nm bandwidth of the MMI splitters. Even though fabrication imperfections and non-ideal behaviour of both waveguide bends and MMIs led to reduced extinction compared to simulations, most devices show in-band extinction exceeding 15 dB. The in-band losses of the most central channels did not exceed 1.5 dB compared to the reference straight waveguide. The designed interleavers can be employed in cascaded configurations to achieve broadband and fabrication tolerant flat-top wavelength (de)multiplexers.

1. INTRODUCTION

Flat-top response of optical filters is highly desirable and often mandatory, especially in telecommunication applications, whenever in-band ripples can cause unwanted signal distortions (e.g. in high-speed links) and/or power variations induced by wavelength drifts of the light sources (e.g. in CWDM systems with no thermal control). A popular simple solution for optical filtering is the unbalanced Mach-Zehnder interferometer (MZI), that can be simply used as an interleaver or as the building block of suitably designed cascaded tree-architectures[1] to realize $1x2^n$ (de)muxes. One main drawback of using simple MZIs is their sinusoidal response, which cannot ensure flat passbands and high extinction ratios. Using suitably designed second order MZIs is instead possible to achieve a flat response[2,3], and this approach has been already exploited to achieve flat-top 1x8 (de)muxes on a submicron silicon photonic platform[1]. An alternative approach can be based on microring-loaded MZIs[2,4], that have the advantage of using just single-stage MZIs, and of having steep roll-off, ensuring significantly higher extinction ratios.

A somewhat different flattening approach has been introduced by Jinguji et al.[5], based on elegant symmetry principles applied to fourth order MZIs. The only drawback was the need for a numerical optimization algorithm to calculate the splitting ratios of the couplers. This limitation has been overcome ten years later[6] based on a powerful geometric representation of 2-port interferometric filters, which not only led to simple analytic formulas for the splitting ratios, but also extended the class of working symmetries.

The aim of this paper is to show how this last design approach can be implemented in the micron-scale silicon platform of VTT, only based on MMI splitters, leading to compact and fabrication tolerant devices. VTT platform is an interesting alternative silicon photonics platform, based on 3 µm thick silicon on insulator (SOI) wafers. Single mode condition is ensured by suitably designed rib waveguides[7], obtained by etching 40% of the silicon layer thickness. Strip waveguides are obtained by etching the remaining silicon through a self-aligned process[8], also ensuring very low loss rib-to-strip converters[9]. Total internal reflection (TIR) in silicon can also be exploited to design and fabricate low loss mirrors for both rib and strip waveguides[10]. All these elements are schematically depicted in Fig. 1.a. A thermal oxidation step is

*silicon.photonics@vtt.fi; phone +358 40 684 9040; fax +358 20 722 7012; www.vttresearch.com

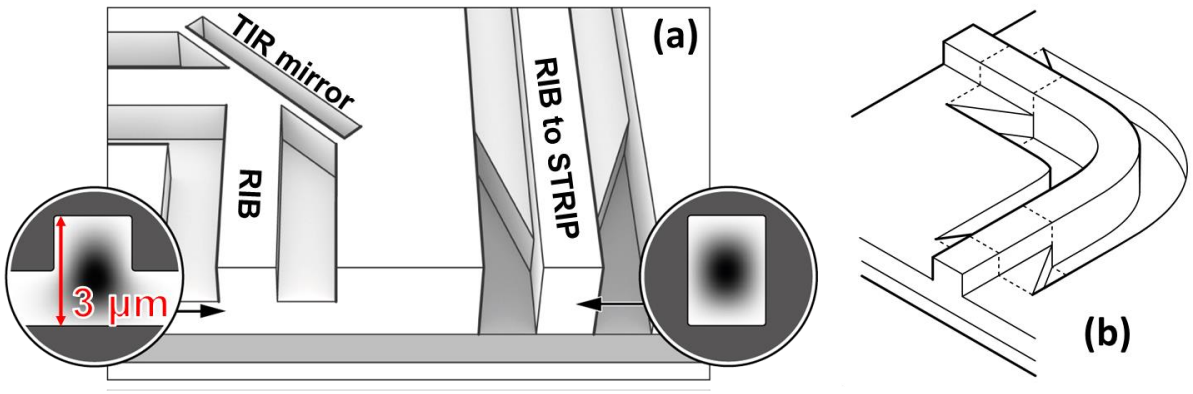

Fig. 1. Exemplified schematics of the VTT silicon photonics platform. a) Rib and strip waveguides with their mode distribution, rib to strip converter, and TIR mirror; b) the Euler bend.

applied to all types of waveguides, leading to propagation losses as low as 0.10 dB/cm in the rib waveguides and 0.13 dB/cm in the strip waveguides. Beside TIR mirrors, micron-scale bends are also possible in multimode strip waveguides, which effectively operate as single-mode, thanks to a recent breakthrough[11,12] (see Fig. 1.b), which led also to a patent[13].

A major challenge for the realization of flat-top higher order MZIs on VTT platform is that they require free choice of splitting ratios, which is typically not possible with ordinary translation invariant MMI splitters. Arbitrary splitting ratios could be in principle achieved using rib waveguide couplers, but they would have a major impact not only on the device footprint, but also on the tolerances to fabrication imperfections, as rib couplers are very sensitive to etch-depth variations of the rib waveguides, which are typically around ± 5% at wafer scale. Rib couplers are typically also wavelength sensitive, which can limit the operation bandwidth of the filters.

For all these reasons, we will instead focus on MMI splitters, which are well known for their relatively broadband operation and tolerance to fabrication errors. We will try to use as much as possible the discrete set of splitting ratios available in standard MMI splitters, and resort to double MMIs[14] only when strictly necessary, so to minimize the number of elements in the filter layout.

In the following we will first introduce in Section 2 the geometrical representation of 2-port systems as a tool to design the flat-top fourth-order MZIs presented in the Section 3. A last section will be devoted to the experimental results and their analysis, followed by conclusions and future perspectives.

2. GEOMETRIC REPRESENTATION OF 2-PORT SYSTEMS

The use of the Bloch sphere representation to treat 2-port interferometric devices has been proposed many times in the literature[15–17], but it didn't gain popularity among the photonics community and, to the best of our knowledge, is not treated in any photonics textbook. A few papers suggested some practical application to the design of flattened directional couplers[18–20] and filters[6]. A rigorous treatment can be found in previous literature. Here we just show in Fig. 2 how to locate the different waveguide modes on the sphere. States where the two waveguides are in-phase are located on one half of the equator, whereas on the other half they are in anti-phase. On the northern (southern) side of the S_1S_3 plane the two waveguides are in quadrature (anti-quadrature). In general, any point can be identified by two angles: θ giving the relative phase and α giving the splitting ratio. In particular, the two states on the S_1 axis represent single waveguide states, and the states on the S_2 axis are the symmetric and anti-symmetric eigenmodes of synchronous directional couplers. In reciprocal systems only rotations about axes belonging to the equatorial plane are allowed, as any rotation about S_3 is non-reciprocal[18]. The action of any 2-port lossless device can be represented on the sphere. A simple example is presented in Fig. 6, that is a MZI with 2π phase shift. The action of a synchronous coupler is represented by a rotation about the axis of its eigenmodes, i.e. the S_2 axis. Having chosen a 50:50 coupler, the first rotation will stop on the S_2S_3 plane. Similarly, a phase shifter is a rotation about the S_1 axis, where its eigenstates are located. The last rotation is again

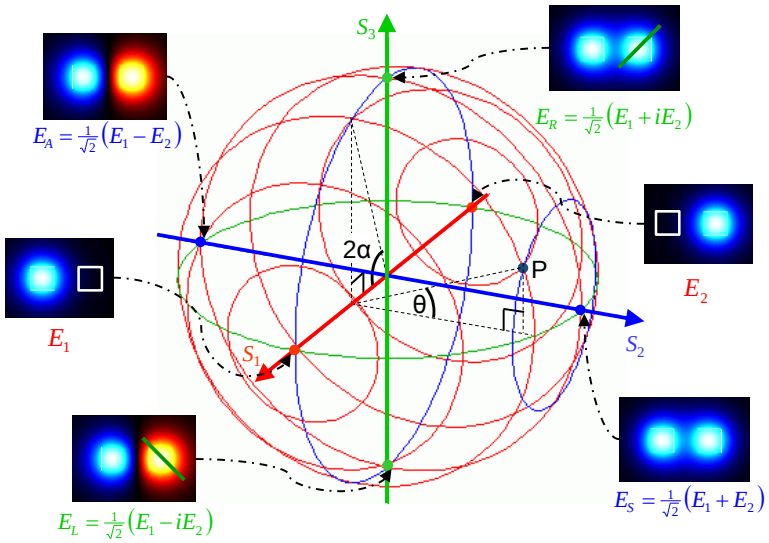

Fig. 2. Geometric representation of 2-port states on the Bloch sphere.

a 90° rotation about S_2 sending the output in the cross port. Noticeably all the MZI output states end up on the equator (i.e. either in phase or in anti-phase), irrespective of the phase shift. Any reciprocal 2-port system can be represented by rotations about axes belonging to the equatorial plane. Axes in between S_1 and S_2 represent asynchronous directional couplers with higher phase shift between the two branches for axes approaching S_2.

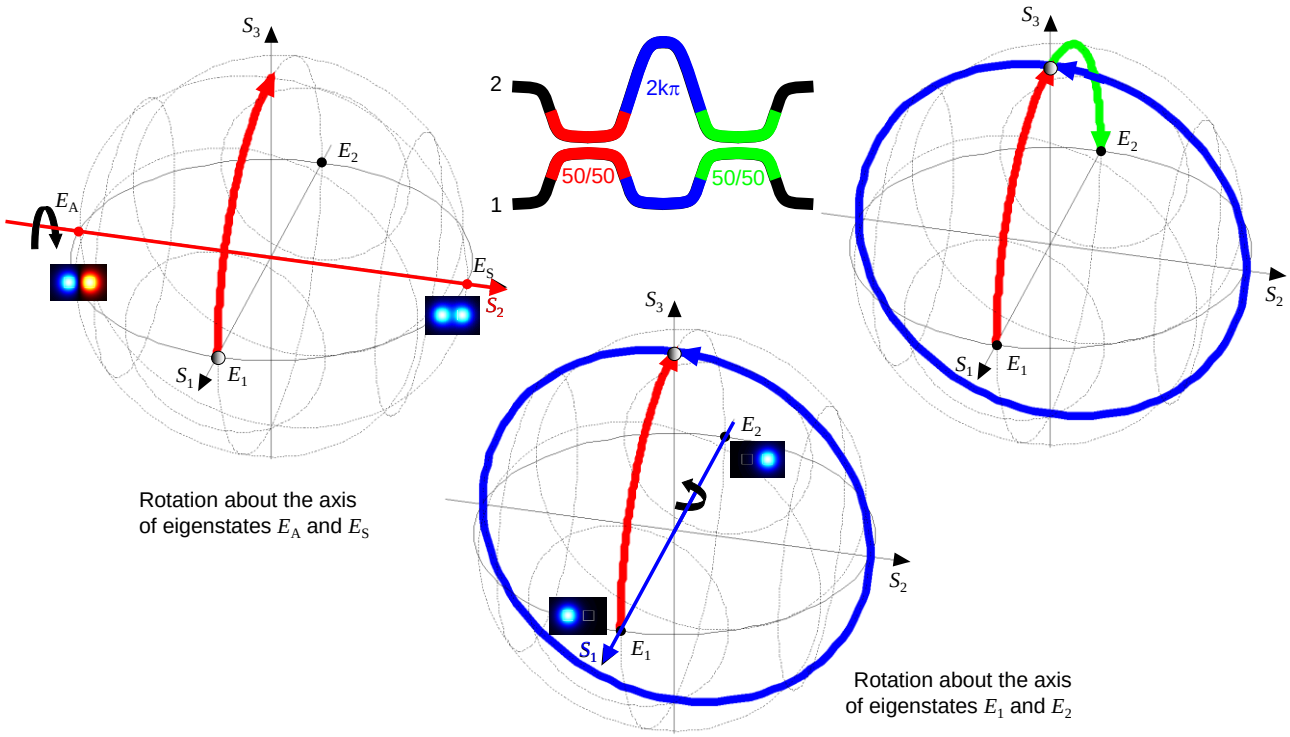

Fig. 3. Example application of the geometric representation to a MZI with 2π phase-shift.

3. FLAT-TOP INTERLEAVERS BASED ON MMI SPLITTERS

As shown in a previous work[6], 4th-order MZIs with flat top response can be designed based on analytic formulas to determine the coupling angles ϕ^A and ϕ^B (see Fig. 4) as follows:

$$\begin{cases} \phi^A = \dfrac{\pi}{16} + (m+k)\dfrac{\pi}{8} \\ \phi^B = \dfrac{\pi}{8} + (m-k-t)\dfrac{\pi}{4} \end{cases} . \tag{1}$$

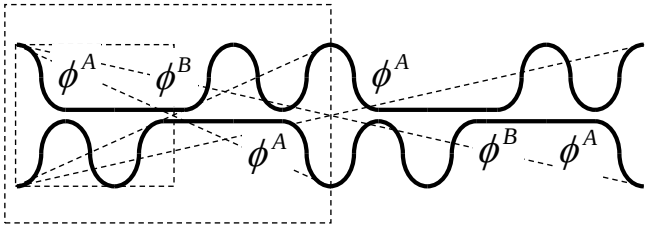

Fig. 4. Schematic of a double point-symmetric configuration, showing the coupling angles ϕ^A and ϕ^B of the couplers.

In particular for $t = k = 0$ and $m = 1$ have $\phi^A = 3\pi/16$ and $\phi^B = 3\pi/8 = 2\phi^A$, which requires a single point-symmetric configuration. As shown in Fig. 5, ϕ^B exactly matches the coupling angle of an 85:15 MMI, while ϕ^A doesn't match any simple MMI design. On the other hand, the two ϕ^A splitters in the middle of Fig. 4 can be combined in a single splitter of angle $2\phi^A = 3\pi/8 = \phi^B$.

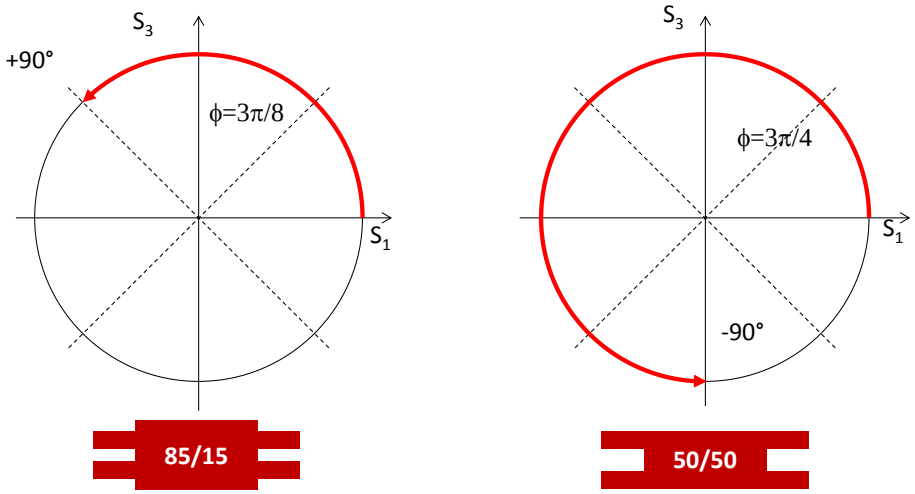

Fig. 5. Geometric representation of the action of 85:15 (left) and 50:50 (right) MMIs on the S_1S_3 plane.

The two ϕ^A splitters at the edges of the filter require instead a double-MMI approach to suitably mimic the action of an equivalent directional coupler. Care must be taken to correct the output phase of the double-MMI, so to make sure that the two ports are in quadrature. In other words, since MZIs end up on the equatorial plane, an additional $\pi/2$ phase shift is needed at the end of the splitter. The action of the resulting double-MMI is shown in Fig. 6, where a $5\pi/8$ phase shift

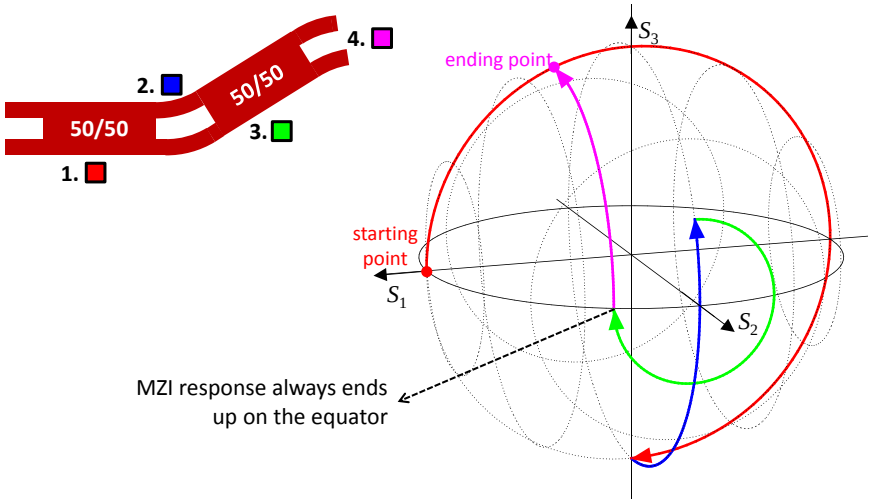

Fig. 6. How to mimic the action of a generic directional coupler based on double MMIs and a final phase shift.

(blue line) between the two MMIs ensures the required splitting ratio. The resulting single point-symmetric structure is depicted in Fig. 7, together with its simulated spectral response in the case of 10 μm extra-length in the MZI arms.

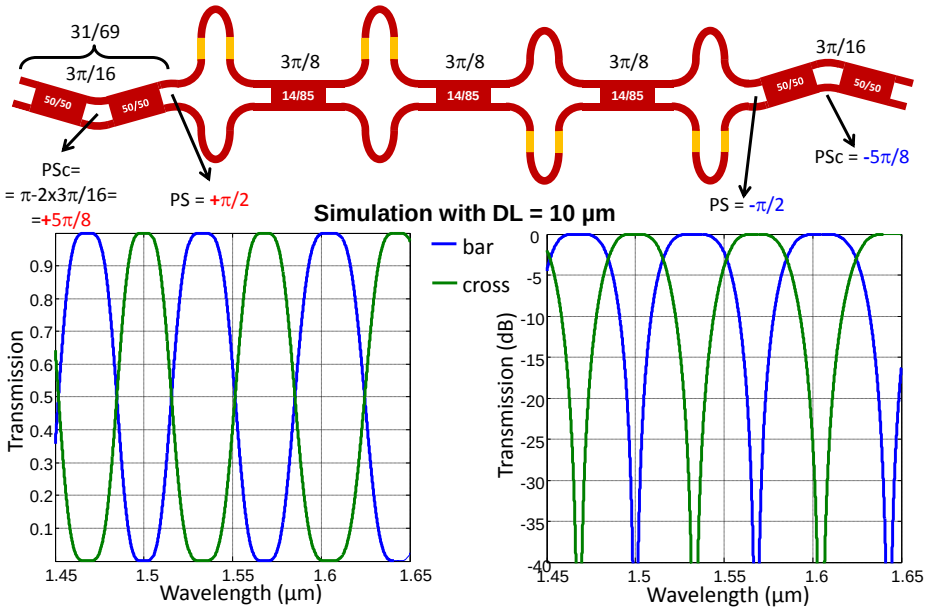

Fig. 7. The proposed flat-top interleaver and its simulated response.

The operation of the filter at nominal wavelengths corresponding to 2π or π phase shifts is shown in Fig. 8. The splitters add up in the first (second) case to send that given wavelength in the cross (bar) port. For the sake of simplicity, the action of the double-MMIs is represented as the equivalent directional coupler. The flat-top response is understood when checking the trajectory on the full sphere corresponding to wavelengths slightly deviating from 2π or π. This is shown in Fig. 9, highlighting how different signs of the phase-shifts nicely cancel out, leading to almost ideal operation. In this case the action of all building blocks of double MMIs is represented.

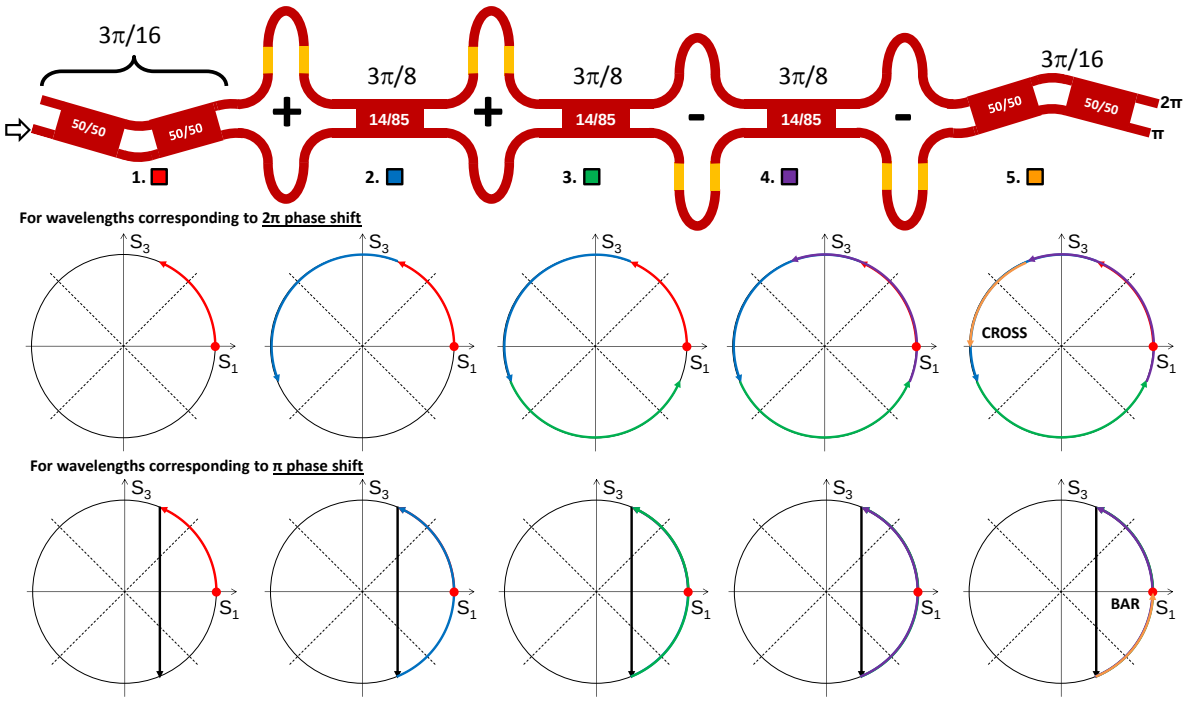

Fig. 8. Operation of the proposed configuration for nominal in-phase and in anti-phase wavelengths.

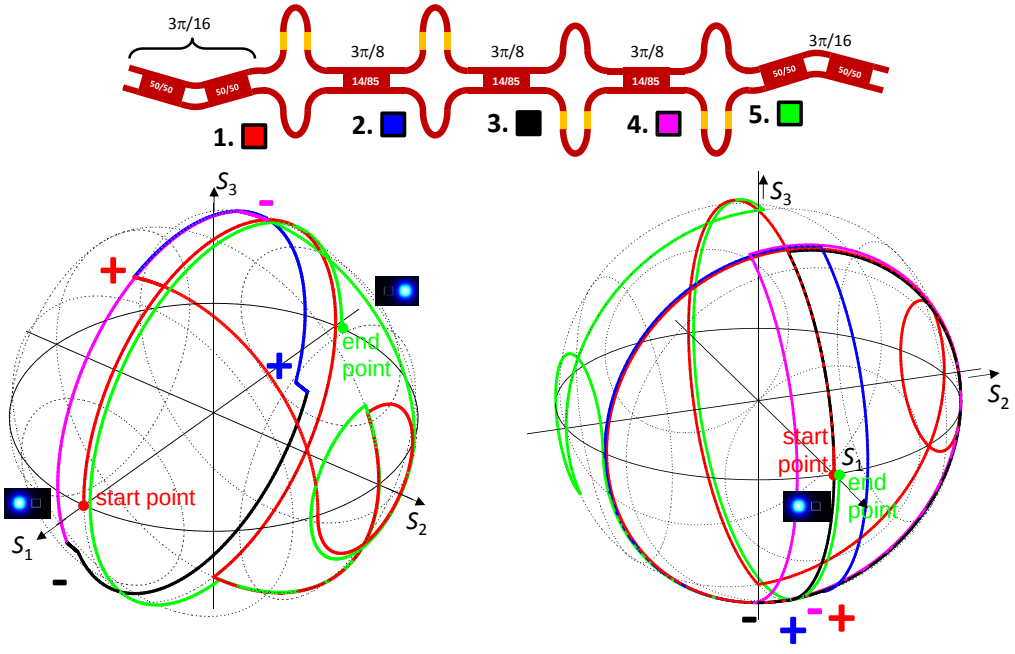

Fig. 9.Geometric representation of the flat top behavior for wavelengths slightly deviating from the in-phase (left) and in-anti-phase (right) condition.

4. FIRST EXPERIMENTAL RESULTS

Fabrication

We have fabricated the designed structures on 3 µm thick SOI wafers based on the well assessed VTT silicon waveguide technology. The devices were fabricated using smart-cut silicon-on-insulator wafers from SOITEC. Initial SOI layer thickness was increased with epitaxial silicon growth. FilmTek 4000 spectrophotometer was used to measure the thicknesses of the SOI layer and the underlying buried oxide. A 500 nm thick Tetraethyl orthosilicate (TEOS) layer was deposited on the wafer in LPCVD diffusion furnace to work as a hard mask in silicon etching. Waveguide fabrication was done using our standard double-masking multi-step process[8]. In the process, two mask layers are passively aligned with respect to each other, and two separate silicon etch-steps form the rib and strip waveguide structures and waveguide facets. Lithography steps were done using FPA-2500i4 i-line wafer stepper from Canon Inc. and pattern transfer to oxide hard mask was done using LAM 4520 reactive ion etcher with CF_4 and CHF_3 chemistry. Waveguides were etched into silicon using Omega i2l ICP etcher from SPTS Technologies. The etching was done with a modified Bosch process[21] using SF_6 and C_4F_8 as etch and passivation gases, respectively, and O_2 as an etch gas to break passivation polymer formed by C_4F_8. After silicon etching, TEOS hard mask was removed with buffered oxide etch (BOE). Hard mask removal was followed by wet thermal oxidation consuming 225 nm of silicon, and thermal oxide removal with BOE. This was done to smoothen the etched surfaces, and to thin the SOI-layer to its final thickness of approximately 3 µm. A 0.17 µm thick silicon nitride layer was then deposited on the wafer with LPCVD as an antireflection coating and to prevent the etching of buried oxide in later oxide wet etch process steps. This layer was patterned in hot phosphoric acid using a hard mask made of 0.25 µm thick LPCVD TEOS patterned with BOE. After silicon nitride layer patterning, 265 nm of LPCVD TEOS was deposited as a cladding layer for the waveguides. As a last step, the oxide layers were removed from the waveguide facets with BOE etch, and wafer was diced into chips.

Characterization

Two kinds of designs has been implemented on mask, each of them with three different extra-length. One is the standard design shown in Fig. 10, together with a measured spectral response of one of the filters. All filters are about 2 mm long and 350 µm wide.

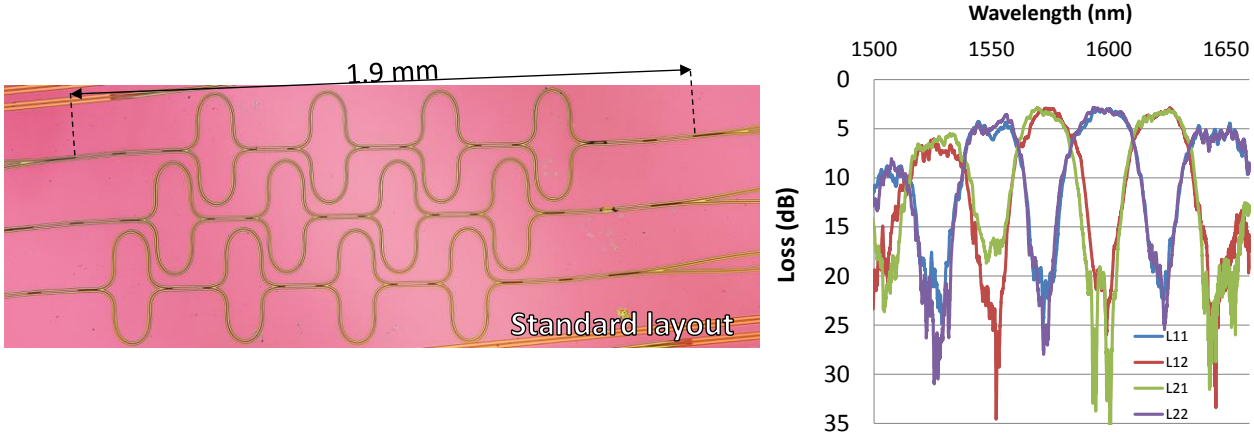

Fig. 10. Micrograph showing the three filters with standard layout and measured spectral response for all ports of one of the devices.

The second type is based on the spiral-like design shown in Fig. 11 - resembling the Superman logo - resulting in a much more compact device. The only drawback of this second approach is that it imposes a lower bound to the minimum possible phase-shift.

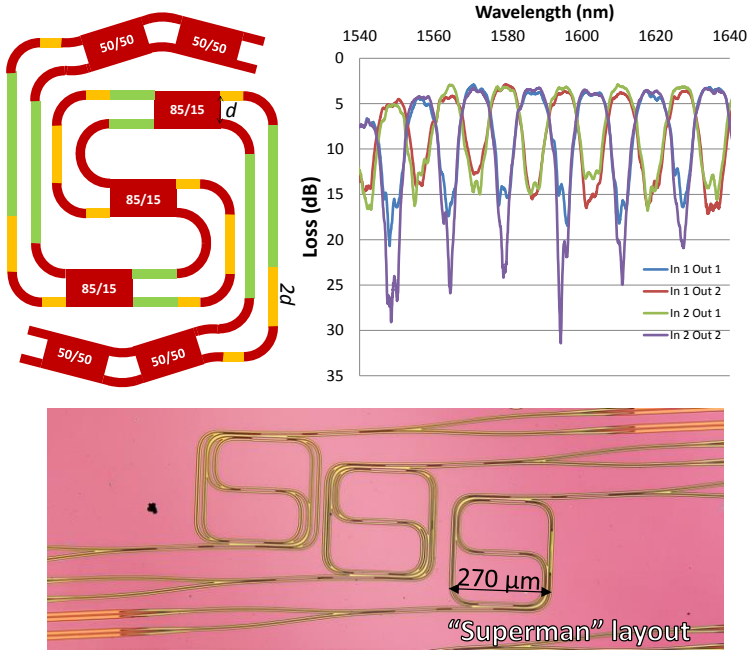

Fig. 11. Schematic of the "Superman" layout, micrograph showing the three implemented filters, and measured spectral response for all ports of one of the devices.

Compared to simulations, both spectra show limited extinction ratio, relatively high losses and asymmetric behavior of the two input ports. When subtracting the 1 dB loss due to input and output fiber coupling to a tapered fiber, best transmission losses are slightly below 2 dB and best extinction ratios not exceed 20 dB. Also loss envelopes, due to limited MMI bandwith, look centered about 1.6 µm wavelength, instead of the designed 1.55 µm. This indicates that the MMI width is wider than designed. Indeed SEM inspection of the fabricated waveguides revealed a linewidth change of about 150 nm in all fabricated structures. This clearly also affected both phase shifters in the double-MMIs, i.e. their splitting ratios and output phases. Considering that no variations of the structures had been put on mask, but only the nominal designs, the linewidth change had a major impact on the filter operation, on transmission losses and extinction ratio. Nevertheless, measured spectra show fairly flat response, demonstrating the robustness of the proposed design to major fabrication errors.

5. CONCLUSIONS

We have designed and fabricated for the first time flat-top MZI filters based on MMI splitters. The design was based on a suitable geometric representation, to find the optimal phase-shift compensation condition. The design was based on three 85:15 MMIs and two double-MMIs, and two different possible layouts have been successfully implemented. Experimental results showed flat-top response, but losses and extinction ratios were non-ideal, mainly due to a major linewidth error in the fabrication process.

REFERENCES

[1] Horst, F., Green, W. M. J., Assefa, S., Shank, S. M., Vlasov, Y. A., Offrein, B. J., "Cascaded Mach-Zehnder wavelength filters in silicon photonics for low loss and flat pass-band WDM (de-)multiplexing," Opt. Express **21**(10), 11652–11658 (2013).

[2] Madsen, C. K., Zhao, J. H., Optical Filter Design and Analysis: A Signal Processing Approach, Wiley (1999).

[3] Li, Y. P., Henry, C. H., Laskowski, E. J., Yaffe, H. H., Sweatt, R. L., "Monolithic optical waveguide 1.31/1.55 mu;m WDM with -50 dB crosstalk over 100 nm bandwidth," Electron. Lett. **31**(24), 2100–2101 (1995).

[4] Oda, K., Takato, N., Toba, H., Nosu, K., "A wide-band guided-wave periodic multi/demultiplexer with a ring resonator for optical FDM transmission systems," J. Light. Technol. **6**(6), 1016–1023 (1988).
[5] Jinguji, K., Takato, N., Hida, Y., Kitoh, T., Kawachi, M., "Two-port optical wavelength circuits composed of cascaded Mach-Zehnder interferometers with point-symmetrical configurations," J. Light. Technol. **14**(10), 2301–2310 (1996).
[6] Cherchi, M., "Design scheme for Mach-Zehnder interferometric coarse wavelength division multiplexing splitters and combiners," J. Opt. Soc. Am. B **23**(9), 1752 (2006).
[7] Soref, R. A., Schmidtchen, J., Petermann, K., "Large single-mode rib waveguides in GeSi-Si and Si-on-SiO2," IEEE J. Quantum Electron. **27**(8), 1971–1974 (1991).
[8] Solehmainen, K., Aalto, T., Dekker, J., Kapulainen, M., Harjanne, M., Heimala, P., "Development of multi-step processing in silicon-on-insulator for optical waveguide applications," J. Opt. Pure Appl. Opt. **8**(7), S455–S460 (2006).
[9] Aalto, T., Solehmainen, K., Harjanne, M., Kapulainen, M., Heimala, P., "Low-loss converters between optical silicon waveguides of different sizes and types," IEEE Photonics Technol. Lett. **18**(5), 709–711 (2006).
[10] Aalto, T., Harjanne, M., Ylinen, S., Kapulainen, M., Vehmas, T., Cherchi, M., "Total internal reflection mirrors with ultra-low losses in 3 μm thick SOI waveguides," Proc SPIE **9367**, 93670B – 93670B – 9 (2015).
[11] Cherchi, M., Ylinen, S., Harjanne, M., Kapulainen, M., Aalto, T., "Dramatic size reduction of waveguide bends on a micron-scale silicon photonic platform," Opt. Express **21**(15), 17814–17823 (2013).
[12] Cherchi, M., Ylinen, S., Harjanne, M., Kapulainen, M., Vehmas, T., Aalto, T., "The Euler bend: paving the way for high-density integration on micron-scale semiconductor platforms," Proc. SPIE **8990**, 899004–899004 – 7 (2014).
[13] Cherchi, M., Aalto, T., "Bent optical waveguide," WO2014060648 A1 (2014).
[14] Cherchi, M., Ylinen, S., Harjanne, M., Kapulainen, M., Vehmas, T., Aalto, T., "Unconstrained splitting ratios in compact double-MMI couplers," Opt. Express **22**(8), 9245–9253 (2014).
[15] Ulrich, R., "Representation of codirectional coupled waves," Opt. Lett. **1**(3), 109 (1977).
[16] Korotky, S. K., "Three-space representation of phase-mismatch switching in coupled two-state optical systems," IEEE J. Quantum Electron. **22**(6), 952–958 (1986).
[17] Frigo, N. J., "A generalized geometrical representation of coupled mode theory," IEEE J. Quantum Electron. **22**(11), 2131–2140 (1986).
[18] Cherchi, M., "Wavelength-Flattened Directional Couplers: A Geometrical Approach," Appl. Opt. **42**(36), 7141 (2003).
[19] Tormen, M., Cherchi, M., "Wavelength-flattened directional couplers for mirror-symmetric interferometers," J. Light. Technol. **23**(12), 4387–4392 (2005).
[20] Paloczi, G. T., Eyal, A., Yariv, A., "Wavelength-insensitive nonadiabatic mode evolution couplers," IEEE Photonics Technol. Lett. **16**(2), 515–517 (2004).
[21] Gao, F., Ylinen, S., Kainlauri, M., Kapulainen, M., "Smooth silicon sidewall etching for waveguide structures using a modified Bosch process," J. MicroNanolithography MEMS MOEMS **13**(1), 013010–013010 (2014).